

Formulating Depth Information in an Image

A. Saadat¹

In conventional imaging systems, the depth difference of two visible points appears as the defocus difference of their images. A monotonic relation between the depth of a set of points and the amount of defocus of their images may be obtained by focusing the camera on closer sets. Measuring depth may lead to measuring defocus at each image point. Generally, a defocusing operator can be modeled as a linear, circular symmetric, low pass, positive and space variant filter. In the approach, proposed here, for solving the depth finding problem, the spatial scope of the defocusing filter is used as a measure of depth, without imposing any restriction on its shape. Through an analytic procedure for finding the scope of the filter at each region of interest, a general criterion for depth will be obtained. Due to the simple relation with the scope of the defocusing filter, the criterion has a mathematically tractable performance. The given relation provides an effective sense of depth information hidden in a simple image of a scene. The problem formulation is such that it points to the conditions which validate the relation.

INTRODUCTION

In conventional imaging systems, the depth difference of two visible points appears as the defocus difference of their images. In a simple analysis, the defocusing effect changes the image of a point to the well-known blur circle with radius proportional to depth [1]. Measuring depth may lead to measuring defocus at each image point. A one to one monotonic relation between the scope of the defocusing filter and depth can be obtained by focusing the camera either on the nearest or the farthest points of a scene. In this paper, it is always assumed that the camera is focused on a point closer than the nearest point of the scene under consideration. The main purpose of this section is to measure the scope of the defocusing filter, as a value proportional to depth, at each image point.

A defocusing operator or blurring function generally can be modeled as a linear, circular symmetric, positive and space variant filter. This model is in harmony with both diffraction and geometric optics. Imposing some certain shapes to the defocusing filter has led to various solutions. A Gaussian filter with spatial variance proportional to depth has been used extensively in the literature. This model, deduced from diffraction optics [2], has not been satisfied generally [3] and is not observed as a proper model [4]. Based

on geometric optics, blur circle or Circ function, with radius proportional to depth, has been used in the spatial domain [5]. Analysing defocused step edge has been investigated previously in [2,6,7]. In [2,6], depth parameter has been obtained from a double differentiation of the intensity image in the neighborhood of vertical edges. Based on the selected model for the defocusing operator, variance in [2,7] or second central moment in [6] have been used as the depth parameter. Through an optimal procedure in [7], inclined step edges, convolved by Gaussian defocus operator, have been used to obtain the model's variance.

In order to distinguish subjective blurring of a scene from that of the defocus effect, at least two images of the scene, corresponding to different operators, will be required. If the scene characteristics are known or all local areas of the scene have the same texture, only a single image will be enough. Each image of a scene contains its own information of depth. This paper is interested in the quality and quantity of depth information in an image. Therefore, it is more concerned about the information contained in a single image. In spite of the simplicity obtained by the models, current methods have led mostly to complex and non-forward heavy optimal calculations. This complexity has not permitted researchers to analyze their own methods. Experimental results have also been expressed mostly in statistical mean forms.

The purpose of this paper is not to introduce a new method and present some simulation results.

1. *Electrical Engineering Department, Sharif University of Technology, Tehran, I.R. Iran.*

What is being sought, however, is the establishment of solid foundation for the problem of extracting the depth of an image, which itself leads to further basic new methods. The analytic approach to the problem will be based on the most general model of the defocusing filter and will not impose any restriction on its shape. Furthermore, any result obtained by implementing a certain model will not be considered. This paper is organized as follows. First, some definitions and theorems, which simplify the later section, will be presented. Then, the problem is formulated. The main idea in the proposed approach is to use the spatial scope of the defocusing filter at each point as a value directly related to depth. Through an analytic procedure, a monotonic relation between the scope of the windowed image in the regions, considered for depth finding, and the scope of the corresponding defocus filter will be derived. Finally, experimental results will be given followed by the conclusion.

DEFINITIONS AND THEOREMS

Let (r, θ) and (ρ, ϕ) be the polar coordinates in the spatial and frequency domains, respectively. The Fourier transform of function $f(r, \theta)$ is denoted by $F(\rho, \phi)$, in which $0 \leq r, \rho < \infty$ and $0 \leq \theta, \phi < 2\pi$. These functions are related by the following Equation [8]:

$$F(\rho, \phi) = \int_0^{2\pi} \int_0^{\infty} f(r, \theta) e^{-j2\pi r \rho \cos(\theta - \phi)} r dr d\theta. \quad (1)$$

When $f(r, \theta) = f(r)$, f is circularly symmetric. Then, F will be also circularly symmetric or $F(\rho, \phi) = F(\rho)$. In this case, f and F are Hankel transform pair related by [8]:

$$F(\rho) = \int_0^{\infty} J_0(2\pi r \rho) f(r) 2\pi r dr. \quad (2)$$

J_0 is the zero order Bessel function of the first kind. Two-dimensional convolution among the circular symmetric functions $f_1(r)$ and $f_2(r)$, which have Hankel transforms $F_1(\rho)$ and $F_2(\rho)$, respectively, is given by [8]:

$$f_1(r) * f_2(r) = \int_0^{\infty} \int_0^{2\pi} r' f_1(r') f_2(R) d\theta dr',$$

$$R^2 = r^2 + r'^2 - 2rr' \cos(\theta). \quad (3)$$

The symbol $*$ denotes two dimensional convolution. The Hankel transform of the resulting function is $F_1(\rho)F_2(\rho)$.

Definition 1

Circular Symmetric Form (CSF) and Normalized Circular Symmetric Form (NCSF)

The CSF of $f(r, \theta)$ is defined as its mean over the range of $0 \leq \theta < 2\pi$ at any r . The resulting function may be denoted by $f(r)$ for simplicity:

$$f(r) = \frac{1}{2\pi} \int_0^{2\pi} f(r, \theta) d\theta. \quad (4)$$

Furthermore, the CSF of $F(\rho, \phi)$ may be shown by $F(\rho)$. The NCSF of a 2-D function is obtained by dividing the CSF of that function by its value at the origin. The NCSF is usually used in the frequency domain. Suppose $F(\rho)$ be the Hankel transform of a positive value function $f(r)$, normalizing $F(\rho)$ means dividing it by its maximum value. This is the result of the following procedure:

$$\begin{aligned} |F(\rho)| &= \left| \int_0^{\infty} J_0(2\pi r \rho) f(r) 2\pi r dr \right| \\ &\leq \int_0^{\infty} |J_0(2\pi r \rho)| f(r) 2\pi r dr \\ &< \int_0^{\infty} f(r) 2\pi r dr = F(0). \end{aligned} \quad (5)$$

The relation $|J_0(x)| < 1$, for any positive real value x , has been used to derive Relation 5.

Definition 2

Mean of a Circular Symmetric Function with the Density of Another Function

The mean of a circular symmetric function $g(r)$ with the density of another function $f(r)$, denoted by $E\{g\}_f$, is defined as:

$$E\{g\}_f = \frac{\int_0^{\infty} g(r) f(r) r dr}{\int_0^{\infty} f(r) r dr} \quad (6)$$

When $f(r)$ is positive, normalizing it through division by its infinite integral produces a probability density function. Note that the integrations in Equation 6 are two dimensional and weighing r is the result of the surface element $2\pi r dr$ in (r, θ) plane.

Definition 3

Scope of a Positive Circular Symmetric Function (PCSF)

The scope of a PCSF $f(r)$ is defined as:

$$d_f = [E\{r^2\}_f]^{1/2}. \quad (7)$$

Note that $E\{r^2\}_f > 0$ guarantees real roots and provides a positive value for d_f . d_f^2 can be interpreted as

the power of the signal having density $f(r)$. Although the CSF of the Fourier transform of an image may not be a positive real value function, it will be seen that under certain conditions, this definition can also be used for that function.

Definition 4

Function's Family (FF)

Functions with a free parameter and independent variable(s) that have similar closed form constitute an FF. Each value of the parameter represents a certain member of the corresponding family. Generally, the Fourier transform of members of an FF is another FF. Gaussian FF is one of the few exceptions here. Variance is the well-known parameter of the Gaussian FF.

The proofs of the following theorems are stated in [9].

Theorem 1

Let $F(\rho, \phi)$ be the Fourier transform of $f(r, \theta)$. The CSFs of $F(\rho, \phi)$ and $f(r, \theta)$ are Hankel transform pair.

Theorem 2

Suppose $f(r)$ and $F(\rho)$ are Hankel transform pair; i) If $f(0)$ is positive and a local maxima of $f(r)$, then $E\{\rho^2\}_F$ will be positive, ii) If $f(0)$ is positive but not a local minima of $f(r)$, then $E\{\rho^2\}_F$ will be non-negative.

The property of a function being Positive And Not having local Minima At the Origin is simply called PANMAO.

Theorem 3

Consider PCSFs $f_1(r)$, $f_2(r)$ and $f_3(r)$ with the corresponding scopes d_{f_1} , d_{f_2} and d_{f_3} , respectively. If $f_1(r) = f_2(r) * f_3(r)$, then the following relation is maintained:

$$d_{f_1}^2 = d_{f_2}^2 + d_{f_3}^2. \quad (8)$$

Theorem 4

Let the certain functions $f(r)$ and $F(\rho)$ be Hankel transform pair. If $f(r)$ is a member of FF denoted by $g(r) = f(ar)$, having Hankel transform $G(\rho)$ and family's parameter a , the product $E\{r^2\}_g E\{\rho^2\}_G$ will be a certain value independent of a .

Comment

This value is called Family's Constant (FC) for $g(r)$ or $G(\rho)$ FF. $f''(0) = 0$ or $F''(0) = 0$ causes $E\{\rho^2\}_G = 0$ or $E\{r^2\}_g = 0$, respectively, resulting in an FC equal to zero.

PROBLEM FORMULATION

The main purpose of this section is to measure the scope of the defocusing filter, as a value proportional

to depth, at each image point. The defocusing process is analyzed in a local area of the scene with a fixed depth or, equally, in a small selected region of the captured image on which the filter can be assumed space invariant. Using the functions:

$$\begin{aligned} s(r, \theta) & : \text{focused image of the scene} \\ i(r, \theta) & : \text{defocused or captured image} \\ h(r, \theta) = h(r) & : \text{defocusing operator} \end{aligned}$$

in the selected region gives:

$$i(r, \theta) = s(r, \theta) * h(r). \quad (9)$$

The corresponding Fourier transforms of the functions are related by:

$$I(\rho, \phi) = S(\rho, \phi)H(\rho). \quad (10)$$

The CSF of Equation 10 can be written as:

$$I(\rho) = S(\rho)H(\rho), \quad (11)$$

where the same symbols were used for simplicity. The Hankel transforms of the functions in Equation 11 are given by:

$$i(r) = s(r) * h(r). \quad (12)$$

In accordance with Theorem 1 and since $I(\rho)$ and $S(\rho)$ are the CSFs of $I(\rho, \phi)$ and $S(\rho, \phi)$, respectively, $i(r)$ and $s(r)$ are also the corresponding CSFs of $i(r, \theta)$ and $s(r, \theta)$.

Applying Equation 9 to the other regions of $s(r, \theta)$, using the $h(r)$ of the selected region, gives a 2-D function $\underline{i}(r, \theta)$ in the entire domain of (r, θ) with the CSF of $\underline{i}(r)$. The function obtained in this way will be equal to the captured image $i(r, \theta)$ only in the regions having the same depth as that of the selected one. This is a simple and useful way to deal with Equation 12 in order to extend it over the entire domain of $s(r)$. This reveals the abilities and outlines the applications of the criterion of depth introduced later. Considering this and taking the Hankel transform of both sides of Equation 12 leads to:

$$\underline{I}(\rho) = S(\rho)H(\rho). \quad (13)$$

According to Theorem 3, the scopes of the functions $\underline{i}(r)$, $s(r)$ and $h(r)$ are related by the following Equation:

$$d_{\underline{i}}^2 = d_s^2 + d_h^2. \quad (14)$$

Considering Definitions 2 and 3, $d_{\underline{i}}$ will be given by:

$$d_{\underline{i}}^2 = \frac{\int_0^\infty r^3 \underline{i}(r) dr}{\int_0^\infty r \underline{i}(r) dr}. \quad (15)$$

Using $s(r)$ or $h(r)$ instead of $\underline{i}(r)$ in Equation 15, d_s or d_h can be obtained in a similar way. Since $s(r)$ and $h(r)$ are positive real value functions, d_s^2 , d_h^2 and d_i^2 give positive scopes for the corresponding functions. Equation 14 demonstrates that the squared scope of the captured image is equal to the sum of the scopes for the defocusing filter (desired value) and the focused image (additive noise component). In analysis the presence of the desired value and noise component in an additive form makes using the appreciable classic knowledge in linear stochastic systems theory possible. Consequently, the problem of finding d_h^2 would have a mathematically tractable solution. Noting that d_s^2 has a fixed value for the image, d_i can be used as a value proportional to depth, which is true for d_h as well.

Using d_i requires integration of $\underline{i}(r)$ over its entire domain. However, \underline{i} is equal to the captured image i only in the regions having the same depth as that of the selected region. In order to use the captured image, windowing it in each region is necessary. For windowing the captured image, a circle with radius r_m contained in the selected region is considered. The origin of coordinates system is chosen as the center of the circle, therefore, the accessible parameter D_i ,

$$D_i^2 = \frac{\int_0^\infty r^3 \underline{i}(r) w(r) dr}{\int_0^\infty r \underline{i}(r) w(r) dr}, \tag{16}$$

can be used instead of d_i . This requires the windowing function $w(r)$ to be zero outside the selected circle or for $r > r_m$.

Through windowing, it is not likely to have a simple relation, such as Equation 14, among D_i and d_h . This violates the additive form of the true relation (between D_i and d_h) and compromises the mathematical tractability of D_i . However, considering the non-zero amount of information saved after any process, such as windowing, D_i provides useful information about d_i and certainly d_h . The following section derives the general relation between D_i and d_h .

RELATION AMONG D_i AND d_h

The scope of PCSF $f(r)$ was defined as d_f . Consider $F(\rho)$ as the Hankel transform of $f(r)$. Furthermore, it is necessary to define the scope of $F(\rho)$. As stated in Theorem 2, if $f(r)$ has local maxima at the origin, then the expression:

$$E\{\rho^2\}_F = \frac{\int_0^\infty \rho^3 F(\rho) d\rho}{\int_0^\infty \rho F(\rho) d\rho}, \tag{17}$$

will be positive and, based on Definition 3, can be assumed as d_F^2 . Here, d_F can be called the scope of

$f(r)$ in the frequency domain, as d_f in the spatial domain. According to Theorem 2, when $f(r)$ has the PANMAO property, d_F will be valid because of the non-negative value. Relation 5 and the fact that $f(r)$ is a positive real value function show that $(F\rho)$ has PANMAO property. This implies that a function has valid scopes, both in the spatial and frequency domains, provided that the function together with its Hankel transform have PANMAO property. This is a unified approach for using the scope of a function both in the spatial and frequency domains.

The greater the scope of a function in the spatial or frequency domain, the smaller the scope of its Hankel transform in the frequency or spatial domain. Generally, for the members of an FF $f(r)$, the scopes d_f and d_F can be related by:

$$d_F^2 = T_f(d_f^2). \tag{18}$$

T_f is a monotonically decreasing function (MDF) and, therefore, invertible on spatial scopes of the members in the FF. Inversion of T or T^{-1} is also an MDF. In the limit case when d_f (or d_F) is zero, the graph of T_f (or T_f^{-1}) approaches the positive part of the vertical (or horizontal) coordinate in the rectangular coordinates system.

Windowing requires use of the function $i_w(r)$,

$$i_w(r) = \underline{i}(r)w(r), \tag{19}$$

instead of $i(r)$, in each region. Taking Hankel transform of both sides of Equation 19 results in:

$$I_w(\rho) = \underline{I}(\rho) * W(\rho). \tag{20}$$

If $\underline{i}(r)$ and $w(r)$ have the PANMAO property, $i_w(r)$ will also have it. Then, the scope of the functions $\underline{I}(\rho)$, $W(\rho)$ and $I_w(\rho)$ will be valid. According to Theorem 3 and Equation 20, corresponding scopes of the functions are related by:

$$d_{I_w}^2 = d_{\underline{I}}^2 + d_W^2. \tag{21}$$

Like Equation 18, each of the three parts in the above equation is an MDF of the corresponding part in the spatial domain. Therefore, Equation 21 can be written as:

$$T_{i_w}(d_{i_w}^2) = T_{\underline{i}}(d_{\underline{i}}^2) + T_w(d_w^2), \tag{22}$$

where T_{i_w} , $T_{\underline{i}}$ and T_w are MDFs of the corresponding scopes of the FFs i_w , \underline{i} and w , respectively. Taking the inversion of T_{i_w} or $T_{i_w}^{-1}$ of both sides of Equation 22 yields:

$$d_{i_w}^2 = T_{i_w}^{-1}[T_{\underline{i}}(d_{\underline{i}}^2) + T_w(d_w^2)]. \tag{23}$$

However, d_{iw} or the scope of $\underline{i}(r)w(r)$ is equal to D_i (Equation 16). Using this and substituting Equation 14 in the above statement gives the following equation:

$$D_i^2 = T_{i_w}^{-1}[T_{\underline{i}}(d_s^2 + d_h^2) + T_w(d_w^2)], \quad (24)$$

$T_{\underline{i}}$, T_w and $T_{i_w}^{-1}$ are MDFs of their arguments. Thus, d_h relates to D_h through a monotonically increasing function (MIF) in Equation 24. Since $w(r)$ is fixed and T_w is bound limited, choosing any windowing function $w(r)$ will not scratch the monotonical form of Equation 24.

In many cases, Equation 24 can be expressed more explicitly, including a case in which the family's parameter (FP) appears as a multiplicand factor for the independent variable. In that case, Relation 18 changes to the following relation in accordance with Theorem 4:

$$d_F = \frac{k_f}{d_f}, \quad (25)$$

where k_f is the FC. The validity of d_f and d_F causes k_f to be positive. Considering Equation 25, Relation 14 can be written as:

$$\frac{k_{\underline{i}}}{d_{\underline{i}}^2} = \frac{k_s}{d_s^2} + \frac{k_h}{d_H^2}, \quad (26)$$

where $d_{\underline{i}}$, d_s and d_H are the scopes of the functions $\underline{I}(\rho)$, $S(\rho)$ and $H(\rho)$, respectively. $k_{\underline{i}}$, k_s and k_h are also the corresponding FCs.

Situations where some of the FCs are zero should be taken into account. The FC of an FF becomes zero when the scope of the family in the spatial or frequency domain is zero. If the scope is zero only in the frequency domain, some parts of Equation 26 will experience $\frac{0}{0}$ ambiguity. If the scope is zero only in the spatial domain, concluding Equation 26 from Equation 14 will not be possible as, by omitting a zero part of Equation 14, it is not possible to get the corresponding non-zero part in Equation 26. If both scopes of the family, in the frequency and spatial domains, are zero, the two problems described above will arise together. These types of functions are called singular points of Equation 26. Therefore, FFs with zero FC are singular points of the relation.

The purpose of using Equation 26 is to find a general rule among the scope of a function and the scopes of its multiplicand factors. There is no reason for singular points to violate a general solution. However, the impossibility of using them, in the middle stages of the process of finding the general solution, is clear. The best way to find the solution to the singular points is direct calculation based on the definitions presented previously. A comprehensive research in [9] indicates conventional cases in which singular points do not

violate the format of the general solution obtained later. Neglecting singular points and dividing both sides of Equation 26 by $k_{\underline{i}}$ leads to:

$$\frac{1}{d_{\underline{i}}^2} = \frac{k_1}{d_s^2} + \frac{k_2}{d_H^2}, \quad (27)$$

in which $k_1 = k_s/k_{\underline{i}}$ and $k_2 = k_h/k_{\underline{i}}$. Because $k_{\underline{i}}$, k_s and k_h all have positive values, k_1 and k_2 are also positive. To remind and emphasize, \underline{I} , S and H are related by:

$$\underline{I}(\rho) = S(\rho)H(\rho). \quad (28)$$

Equations 27 and 28 indicate a relation between the scope of a function and the scopes of its multiplicand factors, which can be extended easily to more than two multiplicand factors. To summarize the conditions for using Equation 28, it should be noted that: 1) Each factor and its Hankel transform should have the PANMAO property and 2) Factors which have zero value FC are the single points of Equation 27.

Now, D_i is the scope of the function $i_w(r)$ with the multiplicand factors $\underline{i}(r)$ and $w(r)$. As explained previously, the PANMAO property is the only requirement for $\underline{i}(r)$ and $w(r)$ to hold the following relation:

$$\frac{1}{D_i^2} = \frac{c_1}{d_{\underline{i}}^2} + \frac{c_2}{d_w^2}, \quad (29)$$

where $c_1 = k_{\underline{i}}/k_{i_w}$ and $c_2 = k_w/k_{i_w}$ are positive value constants. k_{i_w} , $k_{\underline{i}}$ and k_w are FCs of $i_w(r)$, $\underline{i}(r)$ and $w(r)$, respectively. Because $\underline{i}(r)$ is the same as $i(r)$ inside the window, the above requirement should be provided by the captured image in each region. Moreover, since $i(r)$ and $w(r)$ are, generally, positive value functions, the PANMAO constraint can be reduced to the property of "not having a local minima at the origin of the coordinates system selected in each region". This is the only restriction imposed on the image, and also on $w(r)$, for using D_i as a mathematically tractable measure of depth. Single points of Equation 29 are functions with zero value FC. Because factors $\underline{i}(r)$ and $w(r)$ are positive value functions, this will happen if $w''(0) = 0$ or $i''(0) = 0$, in accordance with the comment of Theorem 4. For singular points, D_i should be computed directly from Equation 16.

Substituting Equation 14 in Equation 30 yields:

$$\frac{1}{D_i^2} = \frac{c_1}{d_s^2 + d_h^2} + \frac{c_2}{d_w^2}. \quad (30)$$

This simple closed relation gives an effective sense of depth information hidden in an image. The simple form of the relation saves sufficient mathematical tractability for D_i to analyze its performance against noise and various image textures. The curve shown in Figure 1

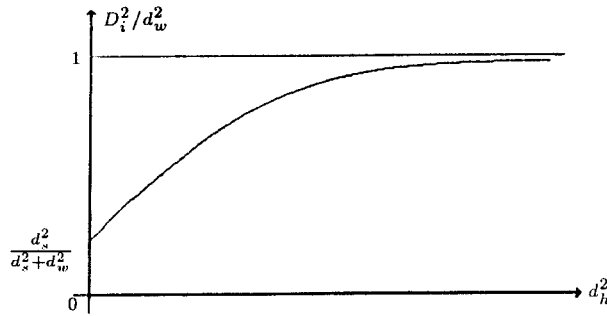


Figure 1. General relationship between D_i^2 and d_h^2 .

depicts D_i^2 , normalized to d_w^2 , versus d_h^2 for $c_1 = c_2 = 1$. It shows a monotonically increasing relation between D_i and depth. As shown in Figure 1 and followed in Equation 30, the curve has an upward trend. This allows lower depths to be resolved more accurately. Also in turn, this is a reason for having low accurate results with deeply defocused images. It should be noted that the scope of $s(r)$ is generally much greater than that of $w(r)$. This forces $d_s^2/(d_s^2 + d_w^2)$, or the initial value, to be close to one. Therefore, normalized D_i^2 will not have a wide range of variations.

EXPERIMENTAL RESULTS

Using edge texture, the ability of D_i in resolving depth was experimentally tested. The experimental equipment used was a black-and-white CCD camera, a frame grabber with 6 bits resolution and a commonly used personal computer for data acquisition and computing D_i . The scene in the experiment composed of a black stripe fixed to a white sheet of paper which was tilted against the camera. The paper was placed in such a manner that the distance from the camera increased linearly from left to right. The camera was focused on an object with a distance less than that of the nearest point of the sheet.

Figure 2 shows the corresponding captured image of the scene. The image has 300 pixels in length. The gradual narrowing of the stripe and its increased blurring from left to right indicate the increase in depth along the edge. To compute D_i along the stripe, all centers of the integrations should be chosen in the lighter part at a fixed distance from the edge. In order to locate the edge, the fact has been utilized that the second order directional derivative of the image, in a direction intersected by the edge, is zero at the intersecting point. For simplicity and for obtaining results that are less dependent on r_m , the performance of $M_i = D_i^2/(r_m^2/2)$, instead of D_i^2 , is considered for the experiment. It should be noted that for images having constant CSF, inside an integration circle with radius r_m , M_i becomes one. Also, d_w^2 is the same as $r_m^2/2$ for the Circ windowing function with radius equal to r_m .

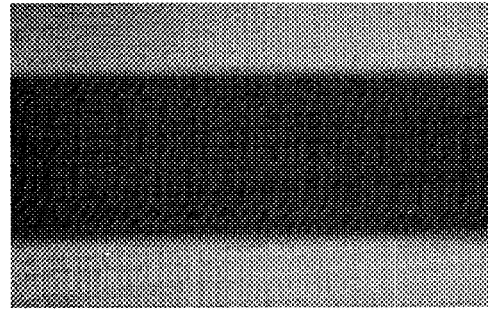


Figure 2. Image of the scene

Figure 3 shows M_i , along the edge, with linear variations in depth. Due to various sources of error in the image, having a monotonically increasing form with a local average of M_i is a desired behavior for resolving depth. The results shown in Figure 3 indicate this capability. There is good agreement between the experimental results and the behavior of normalized D_i^2 , derived generally in the previous section, which is shown in Figure 1.

In Figure 3, the curve with a smaller r_m is above the other one. Furthermore, it is illustrated that two curves with various r_m do not intersect each other and that the initial point of the curve with a smaller r_m , at $d_h = 0$, will be over that of the curve with a larger r_m . Therefore, normalized D_i^2 or M_i is a decreasing function of d_w or r_m at each d_h or depth. As shown in Figure 3, M_i has values near one with a low range of variations. This can also be seen from the theoretical results shown in Figure 1 and discussed previously. Another common feature of theoretical and experimental results is the slightly upward trend for M_i at smaller r_m . This has been shown clearly in Figure 1, which is in agreement with the curve with a smaller r_m in Figure 3. The trend reduces the capability of M_i in resolving depth. Increasing r_m

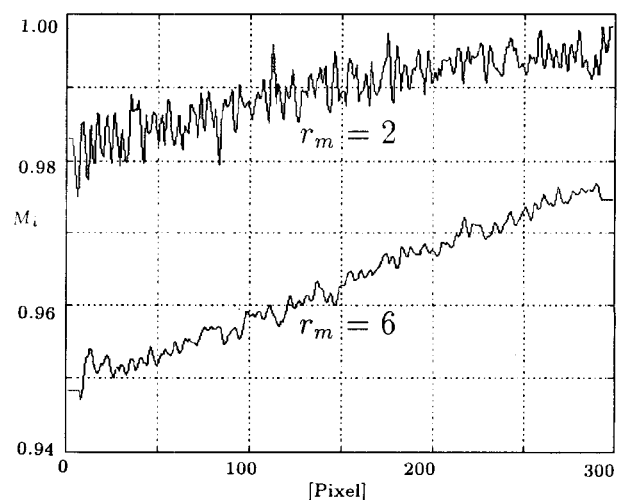


Figure 3. Experimental M_i by linear variations in depth.

improves this capability as the experimental results corresponding to larger r_m are in accordance with reality.

CONCLUSION

Extracting depth information from a scene contained in a simple image was the main aim of the paper. The spatial scope of the defocusing filter has a monotonic relation with depth. Through an analytic procedure, a simple relation between the scope of the captured image and the scope of the defocusing filter, in each region of interest, was obtained. Despite simplicity, the relation exhibits a clear concept of depth information, hidden in a simple image, through embodying it in a closed form. A simple form of the relation encourages sufficient mathematical tractability for the given criterion to analyze its performance. In addition to the mathematically tractable performance of the criterion, it does not require Fourier transform calculations, differentiation, or complex optimal procedures. Error analysis in [9] indicates the high capability of the proposed criterion in resolving depth in a single image. Describing this is beyond the scope of this paper. Furthermore, experimental results were in good agreement with the theoretical ones.

REFERENCES

1. Horn, B.K.P., *Robot Vision*, MIT Press, Cambridge, Massachusetts, USA (1987).
2. Pentland, A.P. "A new sense for depth of field", *IEEE Trans. Pattern. Anal. Machine Intell.*, **PAMI-9**(4), pp 523-531 (1987).
3. Williams, C. and Becklund, O., *Introduction to the Optical Transfer Function*, John Wiley and Sons (1989).
4. Subarao, M. "Efficient depth recovery through inverse optics", in *Machine Vision for Inspection and Measurement*, H. Freeman, Ed., Academic, New York, USA, pp 101-126 (1989).
5. Ens, J. and Lawrence, P. "An investigation of methods for determining depth from focus", *IEEE Trans. Pattern Anal. Machine Intell.*, **15** (2), pp 97-108 (1993).
6. Subarao, M. and Gurunoorthy, N. "Depth recovery from blurred edges", *IEEE Comput. Soc. Conf. Comput. Vision Patt. Recogn.*, pp 498-503 (1988).
7. Lai, S.H., Fu, C.W. and Chang, S. "A generalized depth estimation algorithm with a single image", *IEEE Trans. Pattern Anal. Machine Intell.*, **14**(4), pp 405-411 (1992).
8. Bracewell, R.N., *The Fourier Transform and Its Applications*, New York, McGraw-Hill (1986).
9. Saadat, A., *An Analytic Approach for Finding Depth from a Single Image*, Ph.D Thesis in Farsi, Sharif University of Technology (1997).